

This is to certify that the

dissertation entitled

A QUANTITATIVE ASSESSMENT OF TPP-INDUCED DELAYED NEUROPATHY IN THE RETINA AND LATERAL GENICULATE NUCLEUS OF THE EUROPEAN FERRET (MUSTELA PUTORIUS FURO)

presented by

Lee Lipsitz

has been accepted towards fulfillment of the requirements for

Ph.D. degree in Anatomy

MSU is an Affirmative Action/Equal Opportunity Institution

O-12771

LIBRARY Michigan State University

PLACE IN RETURN BOX to remove this checkout from your record.

TO AVOID FINES return on or before date due.

MAY BE RECALLED with earlier due date if requested.

DATE DUE	DATE DUE	DATE DUE
		

6/01 c:/CIRC/DateDue.p65-p.15

A QUANTITATIVE ASSESSMENT OF TPP-INDUCED DELAYED NEUROPATHY IN THE RETINA AND LATERAL GENICULATE NUCLEUS OF THE EUROPEAN FERRET (MUSTELA PUTORIUS FURO)

By

Lee Lipsitz

A DISSERTATION

Submitted to
Michigan State University
in partial fulfillment of the requirements
for the degree of

DOCTOR OF PHILOSOPHY

Department of Anatomy

2000

ABSTRACT

A QUANTITATIVE ASSESSMENT OF TPP-INDUCED DELAYED NEUROPATHY IN THE RETINA AND LATERAL GENICULATE NUCLEUS OF THE EUROPEAN FERRET (MUSTELA PUTORIUS FURO)

Bv

Lee Lipsitz

Triphenyl phosphite (TPP), an organophosphorous delayed neurotoxicant, has been examined extensively in our lab to assess its degenerative effects on the central visual pathway of the European ferret. Tanaka et al. (1994, 1999) reported an agerelated pattern of fiber and cell body degeneration in TPP-treated animals. progressing from retinal axons and lateral geniculate nucleus (LGN) neurons to visual cortex. These studies, however, did not address whether TPP exposure also results in retinal ganglion cell (RGC) degeneration, nor did they examine quantitatively the degenerative effects in the LGN. The purpose of this study was to quantify the effects of TPP on RGCs and LGN neurons in the ferret, to describe functional deficits associated with TPP exposure using electroretinography (ERG), and to assess changes in whole-brain neurotoxic esterase (NTE); compounds that induce organophosphorous delayed neuropathy typically inhibit NTE. We administered single subcutaneous injections of TPP (1184 mg/kg) to 13 adult ferrets. Nine were examined 5 days after treatment and 4 were examined 7 days after treatment. Five additional ferrets were injected with TPP and NTE analysis was performed 48 hours after treatment (Johnson, 1977). For histological analysis, the fixed retinae were whole-mounted and the brains were sectioned parasagittally (50

μm) using a Vibratome. All tissue was processed using standard histological and analysis techniques. ERGs were recorded with a DTL Plus™ disposable electrode (Retina Technologies Inc., Hixson, TN) over a range of 4.5 log units below maximum intensity up to maximum intensity (2.5 cd-s/m²). RGC counts from matched nasal regions showed significantly fewer (21%) neurons in the TPP-treated ferrets (5d = 282 \pm 52 SD; 7d = 284 \pm 12 SD) compared with normal (359 \pm 42 SD). No significant difference in cell number was found in temporal retina, even though this region contained, on average, 13% fewer ganglion cells in the TPPtreated ferrets (5d = 334 \pm 44; 7d = 357 \pm 39 vs normal = 394 \pm 72). Mean soma size comparisons and cell size distributions for RGCs in both nasal and temporal retina showed no significant differences for any of the animals studied. LGN neurons were significantly smaller (28%) than normal in the TPP-treated ferrets (5d = 155 μ m² ± 23; 7d = 152 μ m² ± 28 vs normal = 214 μ m² ± 9). The cell size distributions for LGN neurons were shifted toward smaller cell sizes in both the 5and 7-day TPP-treated groups compared to normal. There were no functional deficits detected with the ERG as a result of TPP exposure. TPP produced a 75% reduction in NTE activity compared with normal. The results of this study provide for the first time quantitative evidence that exposure to TPP results in severe degenerative changes in both the retina and LGN of the European ferret.

This dissertation is dedicated to the memory of Dr. Duke Tanaka, Jr.

ACKNOWLEDGMENTS

The completion of this dissertation would not have been possible without the support of many individuals. I would like to begin by thanking Dr. Steve J. Bursian, who has been with me since the beginning of my graduate career. Without his support and willingness to help me in any way possible I would not have completed this degree. Thank you to Dr. Arthur J. Weber, who also played a critical role in my obtaining this degree. His unwavering support and assistance on every aspect of this project was instrumental in the completion of this degree. I am grateful that he stepped into the role as my primary advisor after the loss of Dr. Tanaka, Jr. Thank you to the remainder of my graduate committee—Drs. William Falls, Sharleen Sakai, and David Ramsey—for your support and guidance throughout my program. Thank you Dr. Richard Aulerich for your continuing support throughout my graduate career. I am grateful to the Department of Anatomy faculty and staff who saw me through some very difficult times and encouraged me to not give up. Thanks are due to the Graduate School, College of Veterinary Medicine, and the Michigan Agricultural Experiment Station for their financial support to see me through the last years of this degree. And of course thank you to my family and friends, without whom none of this matters.

TABLE OF CONTENTS

LIST OF TABLES	vi
LIST OF FIGURES	vii
INTRODUCTION	1
MATERIALS AND METHODS Subjects and Procedures Histology Tissue Processing	5
Retinal Ganglion Cell Analysis	6 7 8
NTE Assay	10 12
RESULTS	13
Retinal Ganglion Cells	13 13
Quantitative Analyses	13 15 15
Quantitative Analyses	15
ERG Recordings	16
DISCUSSION	18
APPENDIX A: Tables 1–4	29 34
DIDLIOCD ADLY	<i>3</i> 4

LIST OF TABLES

Table 1	The Effect of Triphenyl Phosphite (TPP) on Retinal Ganglion Cell (RGC) Measurements in the European Ferret	29
Table 2	The Effect of Triphenyl Phosphite (TPP) on Lateral Geniculate Nucleus (LGN) Soma Sizes in the European Ferret	30
Table 3	The Effect of Triphenyl Phosphite (TPP) on Whole-Brain Neuropathy Target Esterase (NTE) Activity in the European Ferret.	31
Table 4	Mean ERG Latency and Amplitude Measurement for the STR, a-wave, and b-wave, at Each Stimulus Intensity	32

LIST OF FIGURES

Figure 1	Schematic drawing of the matched nasal and temporal regions of the retina. The boxed regions within each retina represent the sample areas while the arrows represent their approximate projections to the LGN. The filled circle represents the optic disc in each retina. In the LGN laminae C, A, and A1 are labeled as well as the perigeniculate nucleus (P)	34
Figure 2	Photomicrographs of cresyl-violet stained sections from matched nasal regions of the retina in a normal (A) and a TPP-treated (B) ferret. Note the decrease in retinal ganglion cell density in the TPP-treated retina compared to the normal. Scale bar = $50 \mu m$.	36
Figure 3	Histograms comparing the mean number of retinal ganglion cells in matched nasal and temporal regions of the retina in normal and TPP-treated ferrets 5 and 7 days after treatment (* p < 0.05 Kruskal-Wallis w/Mann Whitney). Nasally there were 21% fewer cells in the TPP-treated ferrets than in the normal ferrets, while temporally there were 13% fewer ganglion cells	37
Figure 4	Histograms comparing the mean soma diameters of retinal ganglion cells in matched nasal and temporal regions of normal and TPP-treated ferrets 5 and 7 days after treatment. Mean soma size was similar for all groups (Kruskal-Wallis w/Mann Whitney)	38
Figure 5	Smoothed histograms showing the size distributions of retinal ganglion cells from matched nasal (A) and temporal (B) regions of the retinae in normal and TPP-treated ferrets 5 and 7 days after treatment. The cell size distributions were similar for all groups (Kolmogorov-Smirnov test)	40

Figure 6	Photomicrographs of cresyl-violet stained parasagittal sections of the ferret LGN. (A) Low power (4x) view illustrating the laminar divisions C, A1, A, and the perigeniculate nucleus (P). (B) Low power view of a 5-day post-treatment LGN. Note the pale appearance of the TPP-treated LGN compared to normal. Scale bar = $50 \mu m$. (C) High power (40x) view of neurons in lamina A1 of a normal LGN. (D) High power view of neurons in lamina A1 of a 5-day post-treatment LGN. Note the irregular shaped, fragmented, pale staining, and pyknotic nuclei (arrowheads) in the TPP-treated in comparison to normal. Scale bar = $500 \mu m$	42
Figure 7	Histogram comparing the mean cross-sectional area in LGN neurons from matched regions in lamina A and A1 in normal and TPP-treated ferrets 5 and 7 days after treatment. The mean cross-sectional areas of LGN neurons in TPP-treated ferrets were 30% smaller than those of normal ferrets (* p < 0.05 Kruskal-Wallis w/Mann Whitney)	43
Figure 8	Smoothed histograms comparing the size distributions of neurons from matched regions in lamina A and A1 of the LGN in normal and TPP-treated ferrets 5 and 7 days after treatment. There was a significant shift toward smaller soma sizes in the TPP-treated ferrets compared to normal (* p < 0.05, Kolmogorov-Smirnov test)	44
Figure 9	Corneal ERG responses. (A) Responses from a normal ferret using a DTL fiber electrode at each stimulus intensity on day 1 and day 5. The STR, b-wave, and a-wave are labelled with arrows. The arrowheads point out the artifact. (B) Responses from a day 5 post-treatment ferret using a DTL fiber electrode at each stimulus intensity on day 1 before treatment and day 5 after treatment. The STR, b-wave, and a-wave are labelled with arrows. The arrowheads point out the artifact	46

INTRODUCTION

Organophosphorous compounds (OPs) are carbon-containing chemicals derived from phosphorous acids. Organophosphates are used extensively as insecticides. They are also used as intermediates in the manufacturing of industrial compounds, pharmaceuticals, fire retardants, antifungal agents, and herbicides, and they have been developed as chemical warfare agents (Padilla et al., 1978; Stephans, 1991; Marrs, 1993; US EPA, 1985; Windebank, 1987; Ecobichon, 1994; Ehrich, 1996). Along with these many uses, OPs appear to have several mechanisms by which they can cause toxicity. Organophosphates are anticholinesterase agents and their acute toxic effects are a direct result of interference with cholinergic transmission. Certain OPs also have been implicated in producing organophosphorous-induced delayed neurotoxicity (OPIDN). Although the mechanism has not been elucidated, it appears unrelated to its anticholinesterase activity (Johnson, 1977; Veronesi, 1987; Abou-Donia, 1992; Ecobichon, 1994; Koelle, 1994; Sultatos, 1994; Kang et al., 1995; Richardson, 1995). It is apparent that the broad applications of use and the many as yet unexplained mechanisms of toxicity pose a significant threat to the health of humans and animals.

Clinically, OPIDN is characterized by a delayed onset of ataxia, and subsequent paralysis (Abou-Donia, 1981; Baron, 1981). Exposure to the OP triphenyl phosphite (TPP), an OPIDN compound, results in widespread axonal degeneration in the mammalian and avian central nervous system (Tanaka *et al.*, 1990, 1992, 1994; Varghese *et al.*, 1995a; Lehning *et al.*, 1996). Of particular interest are the degenerative effects TPP has on the visual system of the European

ferret (Tanaka et al., 1990, 1994). The degeneration pattern found in these animals appears to be age-related. Ferret kits 4 weeks of age or younger do not show any evidence of degeneration in the visual pathway as demonstrated by silver-impregnation, even though degeneration is evident in other brain regions. At 5 weeks of age the kits begin to show retinogeniculate axon degeneration, and by 7 weeks of age there is evidence of lateral geniculate nucleus (LGN) cell body degeneration. Ferret kits at 10 weeks of age have degeneration patterns consistent with the adult animal. This includes retinogeniculate axon degeneration, LGN cell body degeneration, and geniculocortical axon degeneration. This sequence of events led Tanaka et al. (1994, 1999) to hypothesize a pattern of anterograde transneuronal degeneration beginning with the retinal ganglion cells, the first-order neurons in the visual pathway. These studies, however, did not examine directly whether TPP produced damage within the retina. Examining the effects of TPP on the retina was one focus of this study.

OPIDN compounds inhibit certain esterases, including neuropathy target esterase (NTE) (Johnson, 1982, 1990). NTE is an enzyme found primarily in nerve tissue, and at present its function is unknown. It is thought that to initiate OPIDN, NTE must go through a two-step process of phosphorylation by the OPIDN compound, followed by cleavage of an alkyl group from the phosphorylated enzyme, a process called aging (Johnson, 1982; Lotti *et al.*, 1984; Berends, 1987; Abou-Donia and Lapadula, 1990; Kamata *et al.*, 1999). It is presumed that NTE must reach a 70% inhibition threshold before clinical signs and neuropathy are observed. At present, the validity of measuring NTE inhibition to identify OPIDN compounds is controversial. Nonetheless, inhibition of NTE in the domestic female chicken

remains the standard test used by the Environmental Protection Agency (EPA) to identify OPIDN compounds (Varghese *et al.*, 1995; Jamal, 1997; Kamata *et al.*, 1999).

Risk assessment is based not only on the mechanism of a toxic compound, but also on the significance of its effects. Determining whether a toxicant alters visual function is an important component of risk assessment. Although it may take some time to elucidate the mechanism of OP neurotoxicity, it is important to establish functional assays that can be performed on humans and animals exposed to these compounds. This information will enhance the possibility of detecting adverse effects at the earliest possible stage of exposure. With respect to the visual system, electroretinograms (ERGs) are used routinely to assess the functional integrity of the retina. The ERG consists of an initial negative deflecting a-wave, followed by positive deflecting b- and c-waves. Recently, a negative component of the ERG, the scotopic threshold response (STR), was described (Sieving, 1986). The STR originates from the inner retina, and may provide functional information regarding either the direct or indirect responses of retinal ganglion cells (Sieving et al., 1986; Sieving and Wakabayashi, 1991; Frishman et al., 1996).

Based on the above information, the 3 main objectives of this study were to:

1) determine whether TPP causes degeneration of ganglion cells in the retina, 2)

quantify the extent of postsynaptic damage also present in the LGN, and 3) establish whether the ERG might serve as a reliable means to document TPP-induced functional deficits. Since the EPA continues to use NTE inhibition as a standard indicator of the ability of organophosphorous compounds to produce OPIDN, and because the effect of TPP on ferret whole-brain NTE activity has not been

examined, a final objective of this study was to determine if TPP causes a reduction in whole-brain NTE activity.

MATERIALS AND METHODS

Subjects and Procedures

Thirty European ferrets (*Mustela putorius furo*), of both sexes, ranging in age from 1 to 3 years old, were used in this study. Ferrets were housed individually in wire cages at the Michigan State University Experimental Fur Farm. Each cage was bedded with excelsior (wood wool), and food and water were available ad libitum. Temperature and humidity were ambient. Experimental ferrets received a single subcutaneous injection of TPP (1184 mg/kg, 97% pure, Aldrich Chemical Co., Milwaukee, WI). Normal ferrets were not injected. The dose of TPP used has been shown previously to cause clinical deficits and neuronal degeneration characteristic of OPIDN in the ferret (Tanaka *et al.*, 1994, 1999). Animals were observed daily for acute systemic effects, such as difficulty in breathing or vomiting, and signs indicative of OPIDN, such as paresis or paralysis. Any animal displaying signs significant enough to compromise its ability to eat or drink was euthanized with an overdose of pentobarbital sodium (> 50 mg/kg).

Histology

Tissue Processing

Seven normal ferrets and 13 TPP-treated ferrets were used for histological analysis of the retina and LGN. Of the TPP-treated ferrets, 9 were examined 5 days after treatment and 4 were examined 7 days after treatment. All animals were first anesthetized with pentobarbital sodium (50 mg/kg) and perfused transcardially with 1.5% paraformaldehyde and 2% glutaraldehyde in a 0.1M phosphate buffer solution

(pH 7.5). The brain and eyes were removed immediately, and the brains post-fixed in the same solution. The anterior segment of each eye was removed and the posterior eyecups then were placed in 0.01 M phosphate buffered saline (pH 7.5). Following 3 hours of post-fixation, the retinae were removed from the eyecup, whole mounted onto glass slides, dehydrated in graded alcohols, defatted, and stained with cresyl violet. The brains remained in fixative for 24 hours. The forebrain, containing the LGN, was sectioned (50 μm) parasagittally using a Vibratome. The sections were mounted onto glass slides, dehydrated in graded alcohols, defatted, and stained with cresyl violet.

Retinal Ganglion Cell Analysis

Retinal ganglion cell measurements were obtained from 6 normal and 11 TPP-treated ferrets. All comparisons were made in matched regions of the nasal and temporal retina. The representation of the visual field on the ferret retina has been defined as 12.4°/mm (Zahs and Stryker, 1985). Using this as a reference, it was possible to transpose the visual field representation in the LGN back to the correct physical location on the retina. The regions of retina examined were located approximately 1.61 mm superior to the optic disc and 2.02 mm away from the optic disc in either the nasal or temporal direction. These retinal regions were selected for analysis because the axons of ganglion cells located here project to that part of the LGN shown previously to undergo TPP-induced degeneration (Tanaka *et al.*, 1994, 1999). In addition, because these regions are located outside the area centralis and visual streak, ganglion cell density and size are relatively constant. Figure 1 shows the locations of the retinal sample regions and their projection patterns to the LGN.

Each retina was analyzed using a microscope-based digitizing system (Minnesota Datametrics, St. Paul, MN). Using a 40x objective, 4 adjacent retinal areas were captured using a high resolution CCD camera (Hamamatsu model C5985) and image analysis software (Image Pro Plus, Media Cybernetics, Inc.). Cells identified within each sample area were used as references to avoid duplicate cell counts. The stage was moved systematically until images from 4 sequential, but separate, retinal areas were captured (total sample area = 0.164 mm²).

Measurements of the cross-sectional areas of ganglion cells displaying clearly visible nucleoli were obtained using the image analysis software. The somal diameters of these neurons then were calculated from the area measurements. Since retinal ganglion cells have highly circular somata, the areal measurements provide a relatively true estimate of cell diameter.

Lateral Geniculate Neuron Analysis

The LGNs of 6 normal and 13 TPP-treated ferrets were examined. Tanaka et al. (1994) reported heavy neuronal degeneration over the full rostral-caudal extent of the ventral region of laminae A and A1. In order to correlate the region of the LGN examined with the retinal areas studied, the known projection pattern of the ferret's visual field within the LGN was used (Zahs and Stryker, 1985; Figure 1). The parasagittal sections (50 µm) were examined light microscopically to describe the degenerative changes present. Cell measurements were made systematically in each ferret beginning at the rostral border of lamina A and moving sequentially to the caudal edge of lamina A1, where it borders with lamina C. If 100 cells were not counted in an initial pass, a second adjacent pass was made across the ventral region

of laminae A and A1. For all LGNs, the cells were drawn at 1000x using a camera lucida. Cross-sectional areas of the drawn cells were determined using a digitizing tablet (Sigma Scan, Jandel Scientific).

NTE Assay

Forty-eight hours after administration of TPP, 5 normal and 5 treated ferrets were sedated with ketamine HCl (11 mg/kg), and then killed by cervical decapitation. The brains were removed quickly, weighed, and frozen on dry ice. Assessment of NTE activity was performed using the method of Johnson (1977). Briefly, whole brains were homogenized in 50 mM Tris buffer (pH 8.0). An aliquot of the homogenate containing 6 mg of brain tissue was incubated with 40 µM paraoxon, or paraoxon plus 50 µM mipafox, in a final volume of 2 mls. Two milliliters of a phenyl valerate solution (1 vol of 15 mg phenyl valerate/ml redistilled dimethylformamide in 30 vol of 0.03% Triton-X 100), was added to each tube. Tubes were incubated at 37°C for 20 minutes. The reaction was stopped by adding 2 mls of 1% sodium dodecyl sulfate solution containing 0.025% 4-aminoantipyrene. One ml of 0.4% potassium ferricyanide then was added for color development. After 30 minutes, absorbance for each tube was read at a wavelength of 510 nm using a spectrophotometer. Enzyme activity was expressed as nmoles phenyl valerate hydrolyzed/min/gram brain. The percent inhibition of NTE was calculated by dividing the difference between the mean enzyme activity measured in normal and TPP-treated animals by that obtained from the brains of normal animals, and multiplying by 100.

Electroretinography

Usable ERG recordings were obtained from 9 of 30 animals after numerous modifications to the system. Baseline ERGs were recorded with varying light intensities immediately before dosing with TPP. After recording, 5 of the 9 ferrets were injected with TPP. The ERG light intensity series then was repeated on all 9 ferrets at 5 days after treatment. Prior to testing, all ferrets were dark-adapted for 1 hour. Under red light illumination, ferrets were sedated with xylazine (2.2 mg/kg), followed by ketamine HCl (11 mg/kg) given intramuscularly, 20 minutes later. Sedation of all ferrets began 20 minutes prior to each ferret's ERG recording session. This was done to reduce any potential variability in ERG recordings arising from different levels of sedation between animals. The pupil of the right eye was dilated with 1% tropicamide HCl (Mydriacyl[®], Alcon Laboratories, Ft. Worth, TX) and the cornea anesthetized with 0.5% proparacaine HCL (Alcaine®, Alcon). The eyelids were held open with sutures, and a recording electrode was placed on the cornea and held in place with a small amount of methylcellulose. Platinum subdermal electrodes (Grass Instrument Co., Cambridge. MA) were used for the differential and ground electrodes (see below for electrode placement). A Ganzfeld stimulator equipped with a xenon bulb (2.5 cd-s/m²) was used to elicit all ERG responses. The light intensity was varied in 0.5 log unit steps using Kodak Wratten neutral density filters over a range of 4.5 log units below maximum intensity up to maximum intensity (2.5 cd-s/m²). A bandpass of 0.3-70 Hz was used to filter the ERG responses. At light intensities ranging from -4.5 log units to -1.0 log unit below maximum intensity, 4 flashes, set 5 s apart, were averaged. The final 2 light intensity settings had an interstimulus time of 30 s between the 4 flashes used for

averaging. Signals were amplified and digitized using the Electrophysiologic

Personal Interfaced Computer-2000 (EPIC-2000, LKC Technologies, Inc.,

Gaithersburg, MD) software package. The ERG recordings then were displayed on
the EPIC-2000 computer monitor, and using the EPIC 2000 software package,
latency and amplitude measurements of the STR, a-wave, and b-wave were made.

All latency measurements were made from the onset of the flash stimulus to the start
of the corresponding response. STR amplitude was measured from baseline to the
lowest point of the STR response, the a-wave amplitude was measured from baseline
to the peak of the a-wave response, and b-wave amplitude measurements were made
from the peak of the a-wave response to the peak of the b-wave response.

Corneal Recording Electrodes

An attempt to record stable ERGs was made using 3 different corneal recording electrodes. Initially, a homemade monopolar contact lens containing a platinum wire loop was placed on the eye with a small amount of methylcellulose for adhesion. With the monopolar system, a differential electrode was placed 1 cm from the lateral canthus of the recorded eye, and a ground electrode was placed over the occipital protuberance of the skull. Recordings obtained with this system were not consistent within the same animal, and it often was difficult to record any response from the retina. In addition, the stimulus produced a significant electrical artifact, usually a large negative potential, that occurred prior to the start of the awave. The second corneal electrode system involved the use of a Burian-Allen bipolar corneal electrode (Hansen Ophthalmic Development Laboratory, Iowa City, Iowa) designed originally for use in the rat. With this electrode, only a ground

electrode was necessary, and it was placed over the hindquarters of the animal in order to minimize any potential electrical interference. Unlike other Burian-Allen corneal electrodes, those designed for rats are not attached to a lid speculum. This is because the rat eye, unlike the ferret eye, protrudes forward enough that keeping the lids open during an ERG recording is not an issue. The Burian-Allen electrodes also are designed differently for each species based on the average curvature of the cornea. This ensures proper contact with the cornea. Proper fit of the Burian-Allen electrode was difficult to achieve on the ferret eye. A lid speculum attachment most likely would have improved stability and enhanced the contact of the Burian-Allen electrode on the cornea. The ERG responses generated with this electrode also were not consistent within the same animal, and often no response from the retina could be recorded. In addition, the large negative potential that was observed with the first electrode system remained. The third ERG electrode tried was the DTL Plus™ disposable electrode (Retina Technologies Inc., Hixson, TN). The DTL electrode is a silver/nylon fiber that is placed across the cornea with an artificial tear solution (Isopto-Tears[®], Alcon). The fiber can be cut appropriately to fit across any size cornea. Since this is a monopolar system, differential and ground electrodes again were used, and placed in the nasal dermis and subdermally over the hindquarters, respectively. The ERG responses obtained using this system were greatly improved over those recorded with the other two systems. ERGs were recorded for all animals, and the response was more consistent within the same animal. However, the negative artifact, although diminished, still was present. Attempts to eliminate this artifact were made by replacing the xenon bulb and by conducting the ERGs in a different recording facility. The artifact never was eliminated fully, and it

interfered with interpretation of the a-wave and the STR. The STR was one of the primary ERG components this study intended to examine.

Statistical Analysis

Comparisons of retinal ganglion cell number and mean cell diameter were made using the Kruskal-Wallis and Mann-Whitney tests (SPSS, Chicago, IL).

Differences in mean soma size in the LGNs of normal and TPP-treated ferrets were compared using one-way analysis of variance (ANOVA; SPSS). The Kolmogorov-Smirnov test for two independent samples was used for comparisons of retinal ganglion cell and LGN cell size distributions (SPSS). Differences in mean latency and amplitude measurements at each light intensity setting for the STR, a- and b-waves were compared using a multivariate ANOVA (SAS, SAS Institute, Cary, NC). In all cases, the level of significance was p < 0.05.

RESULTS

Retinal Ganglion Cells

Oualitative Observations

Photomicrographs of matched regions of the nasal retina of a normal and 5-day post-TPP-treated ferret are shown in Figure 2. Since there were no differences between the 5-day and 7-day post-TPP ferrets, only an example from a 5-day animal is shown for comparison to normal. Light microscopically, there is no evidence of any cellular degeneration, as indicated by pyknotic nuclei, in any of the retinal ganglion cells in the TPP-treated animal. The figure also illustrates that a similar range of cell sizes (large, medium, and small) is present in both the normal and TPP-treated retinae. However, the retina of the TPP-treated ferret shows a clear decrease in ganglion cell density.

Ouantitative Analyses

Table 1 presents the number and mean soma diameters of retinal ganglion cells in the nasal and temporal retinae of normal and TPP-treated ferrets. The number of retinal ganglion cells and the mean soma diameters are greater in the temporal retinae compared to the nasal retinae in normal and TPP-treated ferrets. In the nasal retina there were significantly fewer (21%) neurons in the TPP-treated ferrets (5d = 282 \pm 52 SD; 7d = 284 \pm 12 SD) than in the retina of normal ferrets (359 \pm 42 SD). Cell counts from the temporal retinae of TPP-treated ferrets (5d = 334 \pm 44 SD; 7d = 358 \pm 39 SD) were not significantly different from normal (394 \pm 72 SD), even though this region contained, on average, 13% fewer ganglion cells

in the TPP-treated ferrets. There were no differences in mean somal diameters between any of the normal and TPP-treated ferrets in either the nasal or temporal regions. The histograms in Figure 3 illustrate the decrease in cell number in the TPP-treated ferrets compared to normal. The histograms in Figure 4 illustrate that the mean soma sizes of ganglion cells in both the nasal and temporal regions of the retina were similar for the normal and TPP-treated eyes. The smoothed histograms in Figure 5 compare the size distributions of ganglion cells located in the nasal and temporal retinae of normal and TPP-treated animals. There were no significant differences in the cell size distributions for any of the groups. Nasally the range and mean soma sizes are similar (normal = 6.0-26.4 μ m, 12.3 μ m \pm 0.8 SD vs. 5d = 6.5-27.0 μ m, 13.1 μ m \pm 0.7 SD; 7d = 7.1-22.4 μ m, 12.3 μ m \pm 0.7 SD). The range of soma sizes, and the mean soma sizes, are similar temporally as well (normal = 6.6-26.7 μ m, 13.2 μ m \pm 0.6 SD vs. 5d = 6.5-25.4 μ m, 13.7 μ m \pm 0.8 SD; 7d = 7.0-22.2 μm , 13.0 $\mu m \pm 0.8$ SD). Previously, Vitek et al. (1985) reported retinal ganglion cell soma diameters in the ferret retina; 3-4% of the retinal ganglion cells had somata > 20 µm in diameter, (classified as alpha cells), while the remaining 96-97% of ganglion cells had soma diameters measuring $< 20 \mu m$, (all other cell classes). In the present study, 6% (x = 22) of the ganglion cells in the nasal region sampled had soma diameters > 20 μ m, and 94% (x = 337) had soma diameters < 20 μ m. The percentage of retinal ganglion cells with soma diameters $> 20 \mu m$ decreased to 2% (x = 6) at 5-days after treatment and 0.3% (x = 1) at 7-days after treatment. Similarly, the percent of retinal ganglion cells in the nasal region sampled with soma diameters $< 20 \mu m$ increased to 98% (x = 276) and 99.7% (x = 283) for the 5-day and 7-day post-treatment ferrets, respectively. In the temporal retina the percent of

cells with soma diameters > 20 μ m were 3%, 4%, and 1% for normal, 5-day, and 7-day treatment ferrets, respectively. The percent of cells with soma diameters < 20 μ m were 97%, 96%, and 99% for normal, 5-day, and 7-day treatment ferrets, respectively.

Lateral Geniculate Nucleus

Qualitative Observations

There was histological evidence of degenerative changes in the LGNs of TPP-treated ferrets. Qualitatively there were no apparent differences between the degenerative changes in the 5-day and 7-day post-treatment LGNs. The photomicrographs in Figures 6a (normal) and 6b (7-day post-treatment) show the laminar divisions in parasagittal sections of the LGN. The LGN in the TPP-treated ferret stains less intensely due to the loss of Nissl substance, compared to the normal LGN. The individual cells in the rostral-caudal extent of the ventral region of laminae A and A1 were well defined in the normal LGN (Figure 6c). In comparison, the photomicrograph in Figure 6d illustrates that the neurons in the LGNs of the TPP-treated ferrets are irregular in shape, fragmented, pale staining, and pyknotic.

Quantitative Analyses

The cross-sectional areas of all LGN neurons measured in the normal and TPP-treated ferrets are presented in Table 2, and these data are presented graphically in the histograms of Figure 7. The data show that the mean cross-sectional areas of LGN neurons in both 5- and 7-day TPP-treated ferrets (5d = 155 μ m² ± 23 SD; 7d =

152 μ m² ± 28 SD) are significantly smaller (30%) than those of neurons in normal animals (214 μ m² ± 10 SD). The smoothed histograms in Figure 8 compare the size distributions of LGN neurons measured in the normal and TPP-treated animals. There is a significant shift toward smaller cell sizes for both the 5-day and 7-day post-treatment ferrets compared with normal. The histograms suggest a decrease in the percent of large cells and an increase in the percent of small cells in the LGNs of the 5-day and 7-day post-treatment ferrets.

NTE Assay

TPP had a significant effect on whole-brain NTE activity. NTE activity in TPP-treated ferrets was reduced 75% when compared to normal ferrets (Table 3). Mean NTE activity in the normal ferrets measured 1519 ± 161 nmoles phenylvalerate hydrolysed/min/gram brain and in the TPP-treated ferrets the mean activity measured 371 ± 124 nmoles phenylvalerate hydrolysed/min/gram brain.

ERG Recordings

To aid in the comparison of ERG components, ERG recordings from all 9 ferrets on day 1 were grouped as day 1-normals, recordings from the 4 untreated ferrets on day 5 were grouped as day 5-normals, and recordings from the 5 TPP-treated ferrets were grouped as day 5-TPP animals. Figures 9a and 9b show the ERG recordings from the days 1- and 5-normal and day 1-normal and day 5-TPP-treated ferrets, respectively. The STR, a-, and b-waves, and the recurring electrical artifact are labeled. The electrical artifact is first evident at the lowest stimulus intensity (-4.5 log cd-s/m²) and is visible in day 1-normal, day 5-normal, and day

5-TPP recordings. At each stimulus intensity, the amplitude and shape of the artifact is different in the ERG recordings shown in Figures 9a and 9b. The artifact was present only when the corneal electrode was on the ferret's eye. Despite the unpredictable nature of the artifact, it was small enough that latency and amplitude measurements of the STR and the a- and b-waves still could be made (Table 4). The STR first was detected at the lowest stimulus intensity (-4.5 log cd-s/m²), and was measurable until approximately the onset of the b-wave (-3.0 cd-s/m²). The mean latency of the STR ranged from 45-90 msec for day 1-normals, 60-105 msec for day 5-normals, and 45-90 msec for day 5-TPP ferrets over the intensity series. The maximum amplitude of the STR was 133 μ V, 117 μ V, and 233 μ V for the day 1-normal, day 5-normal, and day 5-TPP ferrets, respectively. The amplitude of the STR in the day 5-TPP recordings was significantly different compared to the day 5normal recordings but not from the day-1 normal recordings. The a-wave was first detected at -2.5 log cd-s/m². The mean latency range of the a-wave was 0-45 msec for all groups, and the maximum amplitude was 433 μ V, 383 μ V, and 483 μ V for the day 1-normal, day 5-normal, and day 5-TPP ferrets, respectively. The b-wave was first detected at $-3.0 \log \text{cd-s/m}^2$. The mean latency of the b-wave ranged from 30-120 msec for day 1-normals, 30-105 msec for day 5-normals, and 30-105 msec for day 5-TPP ferrets. The maximum amplitude of the b-wave was 433 μ V, 383 μ V, and 383 μ V for the day 1-normal, day 5-normal, and day 5-TPP ferrets, respectively. The amplitude of the b-wave in the day 5-normal and day 5-TPP recordings were significantly different compared to the day 1-normal recordings (p < 0.05).

DISCUSSION

In this study we used standard histological techniques to quantify the degenerative effects that TPP has on retinal ganglion cells and their target neurons in the LGN of the European ferret. Electroretinography was employed to describe functional deficits resulting from TPP exposure. The effect of TPP on whole-brain NTE activity also was assessed. The results of this study show that exposure to TPP causes a reduction in the total number of retinal ganglion cells. In addition, TPP exposure results in a decrease in mean LGN soma size in lamina A and A1, as well as a shift in the distribution of LGN neurons toward smaller cell sizes. Functional deficits were not detected with the ERG, as a result of TPP exposure. Finally, TPP exposure produced a 75% reduction in NTE activity compared to control.

This study shows for the first time that TPP, an OPIDN compound, causes severe degenerative changes in the mammalian retina. The reduction in the number of ganglion cells in the retina (Table 1; Figure 3) suggests that TPP exposure results in retinal ganglion cell death. This is consistent with the ability of TPP to induce neuronal cell death in other regions of the visual system, including the LGN and visual cortex (Tanaka, 1994, 1999). Hamm *et al.* (1998) recently reported retinal ganglion cell degeneration in fish embryos exposed to the organophosphate pesticide diazinon, and to diisopropylphosphorofluoridate (DFP), an OPIDN compound. The degenerative effects were more severe in embryos exposed to the OPIDN compound DFP than those exposed to diazinon. To the author's knowledge there are no other reports of retinal ganglion cell degeneration from exposure to an OPIDN compound.

In the nasal retina the reduction in retinal ganglion cell number (21%) was significant. However, in the temporal retina the reduction in retinal ganglion cell number (13%) was not significantly different in TPP-treated ferrets when compared to normals. Although it is difficult to explain why there appears to be a differential effect in the temporal vs nasal retina, it may relate to differences in the proposed mechanism of TPP-induced neuronal death, functional differences of ganglion cells, and the overall size of the cells themselves. It has been suggested that TPP induces cell death by mitochondrial toxicity. In vitro studies with cultured chromaffin cells have shown that TPP causes mitochondrial swelling and inhibition of ATP synthesis (Knoth-Anderson et al., 1993). In vivo studies have shown that TPP decreases mitochondrial metabolic enzyme activity in skeletal muscle (Konno et al., 1989). Mitochondria are the principle organelles responsible for ATP production, through cellular respiration. The number of mitochondria in cells is highly variable and dependent on the metabolic needs of the individual cell (Wheater and Burkitt, 1987). Regional differences in metabolic activity in the central nervous system have been documented by examining mitochondrial number and by measuring cytochrome oxidase (CO) activity, a mitochondrial enzyme important in the production of ATP (Carroll and Wong-Riley, 1984; Kageyama and Wong-Riley, 1982, 1984). Kageyama and Wong-Riley (1984) examined CO activity in the ferret retina and found that ganglion cells of the same size formed two general populations, those whose dendrites and somata stained heavily for CO and those that stained lightly. This suggested that cells of the same size can have different metabolic requirements. They reported that the two populations of cells, those with high metabolic activity and those with low metabolic activity, appear to represent OFF-center and ON-center

ganglion cells, respectively. It is known that each region of the mammalian retina has functionally distinct (ON vs OFF) subsets of ganglion cells (Dowling, 1987). Ganglion cells can be considered either OFF-center or ON-center cells based on their response to changes in illumination (Dowling, 1987). Ganglion cells respond to light from a relatively restricted region of space, referred to as the receptive field. An increase in illumination in the receptive field center of an ON-center ganglion cell will cause this cell to increase its firing rate, whereas an OFF-center ganglion cell responds to a decrease in illumination. The increase in metabolic activity in the OFF-center cells in comparison to the ON-center cells reported by Kageyama and Wong-Riley (1984) suggests that these two cell populations might contain different numbers of mitochondria. Although we did not identify cells based on function, if TPP induces cell death by mitochondrial toxicity and ganglion cells in temporal retina contain, on average, more mitochondria than those in nasal retina, then it is possible that the cells with fewer mitochondria are more susceptible to the same concentration of TPP. Additionally, if there is a threshold at which TPP causes cell death, because of their smaller size, nasal cells may reach this critical threshold sooner than the larger temporal cells. In the present study, we found that, in general, cells are larger in temporal retina compared to nasal retina (Table 1). Fitzgibbon et al. (1996) and Vitek et al. (1985) also reported that in the ferret the cell size distribution shifts toward larger sizes in temporal retina. A differential effect on retinal ganglion cells based on the function and size of the cell might explain why a systemically applied neurotoxicant might not affect all neurons equally.

It has been suggested that retinal ganglion cells die by apoptosis as well as by necrosis (Joo et al., 1999; Bien et al., 1999). Cell death by apoptosis or necrosis has been distinguished based on distinctive histopathologic morphologies. Apoptotic cells tend to shrink while their organelles maintain their integrity until eventually the nucleus fragments. Apoptosis is associated with a minimal inflammatory response. Cells are genetically programmed for apoptotic cell death during normal development and it has been suggested that physiological, pathological, or pharmacological agents can activate these genetic pathways after maturation (Thompson, 1998). Cells that die as a result of necrosis appear swollen. Organelles begin to degenerate and eventually the plasma membrane ruptures. Necrotic cell death causes an inflammatory response (Thompson, 1998; Albensi, 1999). In our examination of retinal ganglion cells exposed to TPP we did not see cellular changes characteristic of necrosis, such as swollen somata, pyknosis, or inflammation. Since it was apparent that TPP exposure resulted in a decrease in the number of retinal ganglion cells, we conclude that this loss was primarily by apoptosis.

In agreement with Tanaka *et al.* (1994, 1999) we found severe neuronal changes in the LGNs of ferrets exposed to TPP. We extended their findings by quantifying the degree of degeneration by measuring LGN soma area. There was no difference in LGN soma size between the 5-day and 7-day post-treatment ferrets, but neurons from both groups of animals were significantly smaller than normal. Because cells in lamina A1 and the ventral region of lamina A are uniform in size (Linden *et al.*, 1981), the inclusion of cells located near laminar borders should not have affected our results.

Based on the results of their previous work Tanaka *et al.* (1994, 1999) hypothesized that the age-related sequence of TPP-induced degeneration seen in the ferret central visual pathway was a result of anterograde transneuronal degeneration. By definition, transneuronal degeneration occurs because the insult has effects across a synapse (Cowan 1970). In order for transneuronal degeneration to be responsible for the TPP-induced degeneration of the ferret visual system, the first-order neuron in the central visual pathway, the retinal ganglion cell, must be affected by TPP exposure, and the synaptic connections between the retina, LGN, and visual cortex must be mature. In the present study, we demonstrated that TPP affects the retinal ganglion cells in adult ferrets and we can assume that the synaptic connections along the central visual pathway in an adult are mature. These findings provide support for Tanaka *et al.*'s hypothesis of anterograde transneuronal degeneration. It is possible that the age-related pattern seen by Tanaka *et al.* (1994, 1999) was due to the immaturity of the synaptic connections along the central visual pathway.

It is known that the ferret visual system undergoes a significant period of postnatal development during the first 4-5 weeks of age (Greiner and Weidman, 1981; Linden et al., 1981; Peduzzi, 1988; Jackson et al., 1989; Hutchins and Casagrande, 1990; Voigt et al., 1993; Wong et al., 1993). Synaptic connections within the retina are not fully developed until at least 30 days of age, which suggests that the retinal circuitry is not functionally mature until then. Retinal afferents, initially widespread at birth, segregate into ipsilateral and contralateral projection patterns within their respective LGN territories by 15-21 days of age. Lamination of the LGN begins at 7-14 days after birth, achieving adult-like architecture by 35-40

days, after the retinal circuitry has matured. In visual cortex, formation and development of synapses in all 6 cortical layers occur by 4 weeks of age. If the retinal circuitry, retinal afferents, and LGN lamination patterns are not mature until 35-40 days of age, it is possible that retinogeniculate connections are not mature. Without a mature synapse transneuronal degeneration would not be present at these earlier ages. It would be necessary to examine the retinal ganglion cells of ferrets prior to the onset of retinogeniculate axon degeneration and to examine the retinogeniculate synapse maturity to further investigate the age-related sequence of degeneration reported by Tanaka *et al.* (1994, 1999).

It is important to note that regardless of the anatomical changes we found in the retina as a result of TPP exposure, we found no functional deficits that could be detected using the ERG. The origins of the a- and b-waves and the STR differ and have been well documented. Briefly, the a-wave originates from the activity of the photoreceptors (Brown and Wiesel, 1961; Dowling, 1987) while the b-wave is a direct result of ON-bipolar cell activity (Tian and Slaughter, 1995). Of particular interest in the present study was the STR response, since our anatomical analysis focussed on ganglion cells in the retina.

The STR was first described by Seiving *et al.* (1986), and it is thought to originate from either direct or indirect amacrine cell (amacrine cells synapse on retinal ganglion cells), or retinal ganglion cell activity. The STR can be eliminated when animals are given an intravitreal injection of aspartate (Wakabayashi *et al.*, 1988) since aspartate blocks the synaptic transmission between the photoreceptors and the horizontal cells (Dowling and Ripps, 1972). Furthermore, Bush *et al.* (1995) found that the STR remained in rats even after significant losses in photoreceptors.

Frishman *et al.* (1996) recently reported that the STR has a fast component, arising from amacrine cells, and a slow component, arising from retinal ganglion cells. Although many questions remain regarding the origin of the STR, and what the STR means with respect to retinal function, the present study suggests that retinal ganglion cell degeneration, as a result of TPP exposure, does not affect the STR response significantly. Either the STR is not retinal ganglion cell dominated or ganglion cell numbers can be reduced significantly without affecting the STR.

The results of the ERG recordings do not indicate a treatment effect. Even though the waveform variability and artifact were present, and the artifact was unpredictable, it appears from Figure 9a and 9b that the tracings are affected relatively equally. Figure 9a shows the waveform variability in ERG response that can be seen between the day 1-normal recordings and the day 5-normal recordings. It is apparent that the amplitudes are smaller in the day 5-normal recordings compared to the day 1-normal recordings, although the overall shapes of the recordings are similar. The variability in ERG responses was a technical problem that never was resolved and probably is partially related to the corneal electrode that was used. The DTL electrode is a thread composed of many silver-coated nylon fibers that are placed over the cornea. It is possible that some of the fibers did not lay flat against the cornea or were damaged when the thread was adapted to the smaller eye of the ferret. Other investigators have reported similar problems with the variability of ERG recordings in the same and in different animals using the DTL fiber electrodes (Frishman et al., 1996; Paul Sieving personal comm.).

A second technical problem encountered with the ERG recordings was the presence of an electrical artifact. The artifact was unpredictable, it did not

consistently increase or decrease as the stimulus intensity increased, and it reversed polarity at random stimulus intensities. The origin of the artifact likely arose from the corneal electrode for two reasons. First, the artifact was considerably diminished in amplitude as each new electrode system was used, and second, the artifact was only present when the corneal electrode was on the eye. Even though the presence and shape of the artifact was random, it appears that it has a very short latency and disappears quickly. Typically the a-wave of the ERG is a very fast response occurring within 10 msec (Wakabayashi et al., 1988). Similarly the STR also is a rapid response occurring within 75 msec (Wakabayashi et al., 1988; Sieving and Wakabayashi, 1991; Bush et al., 1995; Frishman et al., 1996). The b-wave has a longer latency than the a-wave or STR, occurring within 100 msec (Sieving and Wakabayashi, 1991). Although we did not measure the latency of the artifact it can be seen in Figures 9a and 9b that it also is relatively short, and thus could potentially affect the a-wave but probably not the b-wave and the STR. Regardless, of the technical difficulties, there still did not appear to be any evidence of functional deficits as a result of TPP exposure.

Previous studies have reported changes in a-wave and b-wave latencies and amplitudes as a result of exposure to organophosphorous compounds. Imai *et al.* (1974, 1983) exposed rats to fenthion, a non-OPIDN compound, and found that at low doses the latency of the a-wave was reduced and the amplitudes of the a- and b-wave were increased. At higher doses the reverse was true, the latency increased and the amplitudes decreased. Yoshikawa *et al.* (1990) exposed rats to 5 different non-OPIDN compounds. They found increases and decreases in latency and

amplitude measurements of the a- and b-wave that were dependent on which compound the animals were exposed to. Kreft *et al.* (1985) exposed trout to an OPIDN compound and found an increase in a-wave amplitude and a decrease in b-wave amplitude. Because the results of these studies are equivocal they have generated some controversy over the role of OPs in ocular toxicology. This in part has led to the re-evaluation of these compounds by the EPA (Boyes *et al.*, 1994).

Finally, this study measures for the first time the TPP-induced inhibition of NTE in the ferret. Our results show inhibition in excess of the threshold currently used by the EPA, as an indicator of OPIDN. Varghese *et al.* (1995b) have reported NTE inhibition below the 70% threshold in Japanese quail exposed to TPP, yet these quail had clinical signs and neuropathology consistent with OPIDN. Whether the differences are due to species variations or not, the EPA continues to use inhibition of NTE in hens as a biomarker. Clearly this may no longer be the most accurate assay.

In summary, the results of this study provide for the first time quantitative evidence that exposure to TPP results in severe degenerative changes in both the retina and the LGN of the European ferret, as well as a significant inhibition of NTE activity. Furthermore, by documenting degeneration in the retinal ganglion cells we have provided further evidence that the TPP-induced degeneration previously described by Tanaka *et al.* (1994, 1999) in the LGN and visual cortex may be a result of anterograde transneuronal degeneration originating at the level of the retinal ganglion cells. TPP exposure does not result in functional deficits that can be detected using the ERG, even though there is retinal ganglion cell degeneration.

APPENDICES

APPENDIX A

Tables 1-4

Table 1. The Effect of Triphenyl Phosphite (TPP) on Retinal Ganglion Cell (RGC) Measurements in the European Ferret.

		Na	sal retina	Temporal retina	
Animal ID	Treatment (days post-nimal ID treatment)		RGC # of diameters ^a RGC (μm)		RGC diameters ^a (μm)
NF55	Normal			279	14.01 ± 2.27
NF13	Normal			377	13.68 ± 2.75
NF52X	Normal	414	11.09 ± 2.32	497	12.18 ± 2.09
NF50X	Normal	370	12.67 ± 2.63	434	13.28 ± 2.57
NF28	Normal	335	12.61 ± 2.64	376	13.19 ± 2.63
NF38	Normal	317	12.85 ± 2.59	403	13.18 ± 2.91
Mean ± SD		359 ±	12.31 ± 0.82	394	13.25 ± 0.62
NF36	TPP(5)	244	13.23 ± 2.41		·
NF41	TPP(5)	243	13.50 ± 2.26	333	13.48 ± 2.34
NF10	TPP(5)	287	12.84 ± 2.62	348	13.49 ± 2.70
NF25	TPP(5)	309	13.61 ± 3.24	298	14.37 ± 3.22
NF5	TPP(5)	252	12.63 ± 2.09	317	13.78 ± 2.35
NF52	TPP(5)	209	13.90 ± 2.40	295	14.62 ± 2.75
NF54	TPP(5)	331	11.83 ± 1.90	415	12.27 ± 2.37
Mean ± SD		282	13.08 ± 0.70	334	13.67 ± 0.83
NF33	TPP(7)	278	13.04 ± 1.73	328	14.00 ± 2.03
NF56	TPP(7)	302	12.70 ± 2.06	320	13.18 ± 1.92
NF9	TPP(7)	284	11.76 ± 1.88	393	12.56 ± 2.54
NF7	TPP(7)	274	11.61 ± 2.01	390	12.13 ± 2.09
Mean ± SD		285	12.28 ± 0.70	358	12.97 ± 0.81

^aData presented as mean ±SD. ^bSignificantly different from normal (p<0.05).

Table 2. The Effect of Triphenyl Phosphite (TPP) on Lateral Geniculate Neuron (LGN) Soma Sizes in the European Ferret.

	Treatment	Mean LGN soma size ^a		
Animal ID	(Days post-treatment)	(μm²)		
NF55	Normal	229 ± 112		
NF12	Normal	201 ± 93		
NF52X	Normal	214 ± 118		
NF50X	Normal	217 ± 96		
NF28	Normal	219 ± 118		
NF38	Normal	206 ± 102		
Mean ± SD		214 ± 10		
NF24	TPP(5)	178 ± 99		
NF32	TPP(5)	182 ± 82		
NF36	TPP(5)	176 ± 97		
NF41	TPP (5)	162 ± 67		
NF10	TPP(5)	121 ± 87		
NF25	TPP(5)	171 ± 116		
NF5	TPP(5)	143 ± 78		
NF52	TPP(5)	132 ± 67		
NF54	TPP(5)	131 ± 57		
Mean ± SD		155 ± 23 ^b		
NF33	TPP(7)	184 ± 76		
NF56	TPP(7)	168 ± 82		
NF9	TPP(7)	124 ± 42		
NF7 TPP(7)		134 ± 53		
Mean ± SD		152 ± 28^{b}		

^aData presented as mean \pm SD.

^bSignificantly different from normal (p < 0.05).

Table 3. The Effect of Triphenyl Phosphite (TPP) on Whole-Brain Neuropathy Target Esterase (NTE) Activity in the European Ferret.

Treatment	Whole-brain NTE activity ^a	% Inhibition	
Normal	1519 ± 161 ^b		
TPP	371 ± 124^{b}	75	

^aActivity expressed as nmoles phenylvalerate hydrolysed/min/gram brain.

^bData presented as mean ±SD.

Table 4. Mean ERG Latency and Amplitude Measurement for the STR, a-wave, and b-wave, at Each Stimulus Intensity.

	Day 1 - normal		Day 5 - normal		Day 5-TPP	
Stimulus intensity (log cd/s/m²	Latency ^a (msec)	Amplitude a (μ V)	Latency (msec)	Amplitude (μV)	Latency (msec)	Amplitude (μV)
-4.5	75 ± 34	71 ± 37	83 ± 11	83 ± 24	84 ± 8.2	113 ± 74
-4.0	69 ± 31	86 ± 49	83 ± 11	117 ± 10	75 ± 10	150 ± 59
-3.5	60 ± 29	81 ± 44	90 ± 21	117 ± 47	60 ± 20	133 ± 54
a-wave						
-2.5	26 ± 14	89 ± 52	23 ± 15	46 ± 34	25 ± 11	97 ± 14
-2.0	23 ± 15	98 ± 33	26 ± 14	50 ± 14	25 ± 11	93 ± 25
-1.5	15 ± 17	132 ± 35	19 ± 8	83 ± 54	10 ± 7	123 ± 42
-1.0	11 ± 8	211 ± 37	8 ± 9	121 ± 21	5 ± 8	213 ± 100
-0.5	8 ± 9	315 ± 50	16 ± 1	213 ± 93	7 ± 13	317 ± 128
0	8 ± 9	343 ± 60	10 ± 9	272 ± 139	0	377 ± 98
b-wave ^c						
-3.5	75 ± 44	112 ± 68	49 ± 57	108 ± 96	72 ± 44	53 ± 49
-3.0	60 ± 21	219 ± 90	83 ± 19	117 ± 41	81 ± 13	123 ± 101
-2.5	41 ± 14	324 ± 86	34 ± 12	217 ± 45	63 ± 16	227 ± 133
-2.0	38 ± 15	324 ± 76	41 ± 8	258 ± 69	54 ± 8	233 ± 115
-1.5	49 ± 28	259 ± 77	38 ± 9	229 ± 103	48 ± 7	183 ± 76
-1.0	38 ± 9	294 ± 74	41 ± 8	233 ± 62	42 ± 7	220 ± 49
-0.5	34 ± 8	302 ± 86	41 ± 8	267 ± 43	45 ± 11	230 ± 85
0	34 ± 8	376 ± 59	40 ± 9	294 ± 77	51 ± 8	273 ± 80

^aData presented as mean \pm SD.

^bDay 5-TPP amplitude measurements are significantly different from Day 1-normal (p < 0.05).

 $^{^{\}circ}$ Day 5-normal and Day 5-TPP amplitude measurements are significantly different from Day 1-normal (p <0.05).

APPENDIX B

Figures 1-9

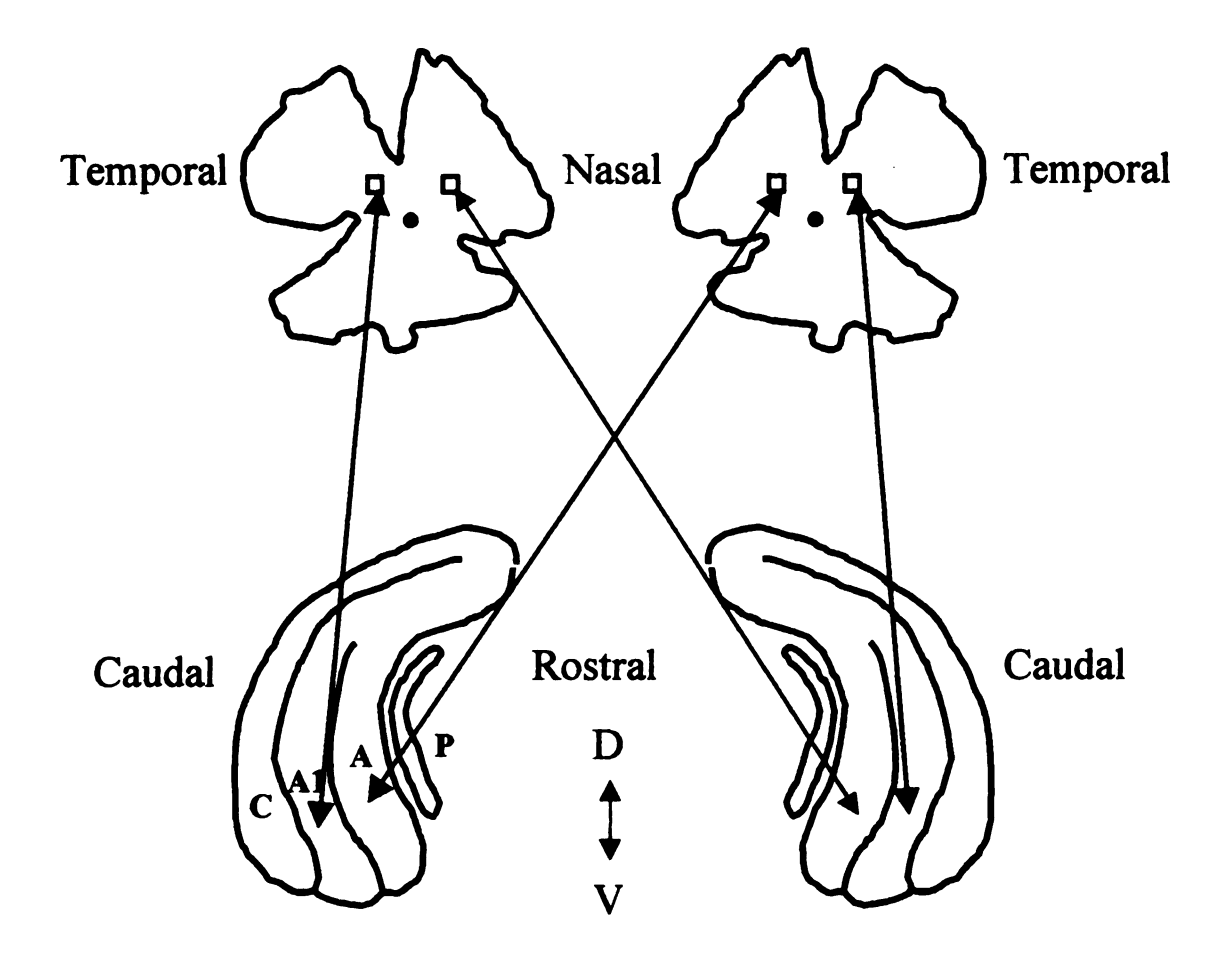
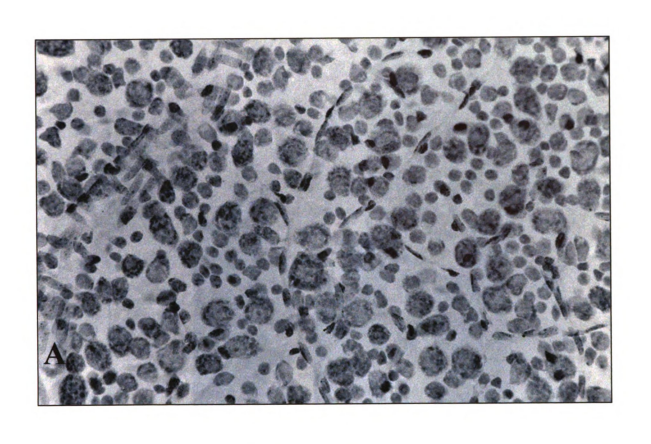
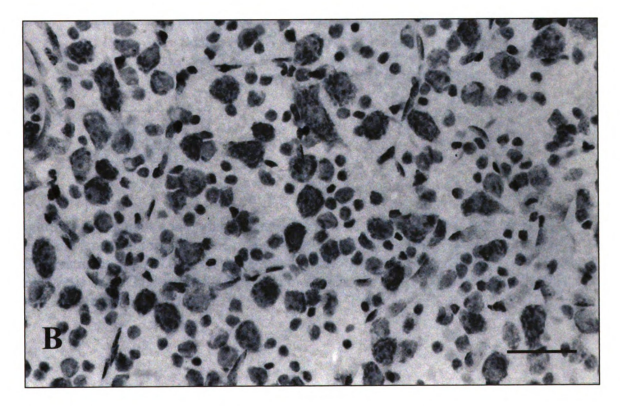


Figure 1. Schematic drawing of the matched nasal and temporal regions of the retina. The boxed regions within each retina represent the sample areas while the arrows represent their approximate projections to the LGN. The filled circle represents the optic disc in each retina. Laminae C, A, and A1 are labeled as well as the perigeniculate nucleus (P).

Figure 2. Photomicrographs of cresyl-violet stained sections from matched nasal regions of the retina in a normal (A) and a TPP-treated (B) ferret. Note the decrease in retinal ganglion cell density in the TPP-treated retina compared to the normal. Scale bar = $50 \mu m$.





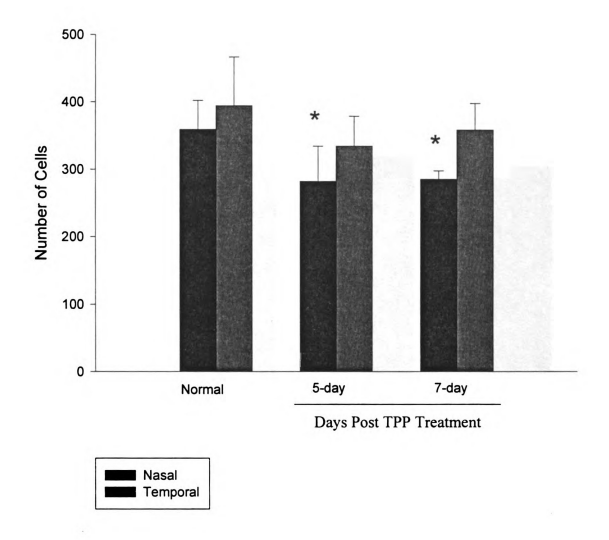


Figure 3. Histograms comparing the mean number of retinal ganglion cells in matched nasal and temporal regions of the retina in normal and TPP-treated ferrets 5 and 7 days after treatment (* p < 0.05 Kruskal-Wallis w/Mann Whitney). Nasally there were 21% fewer cells in the TPP-treated ferrets than in the normal ferrets, while temporally there were 13% fewer ganglion cells.

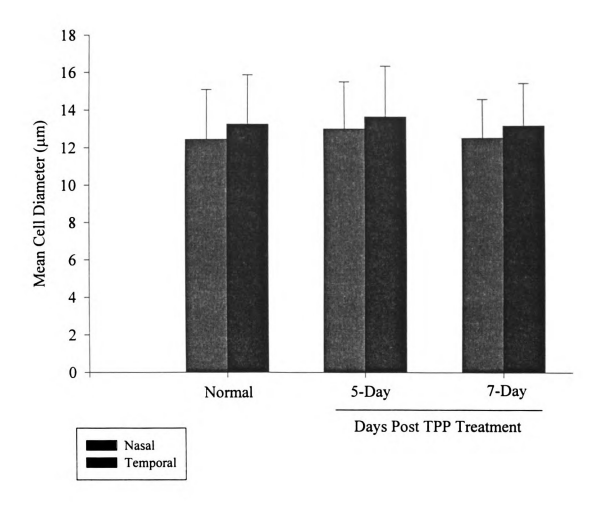
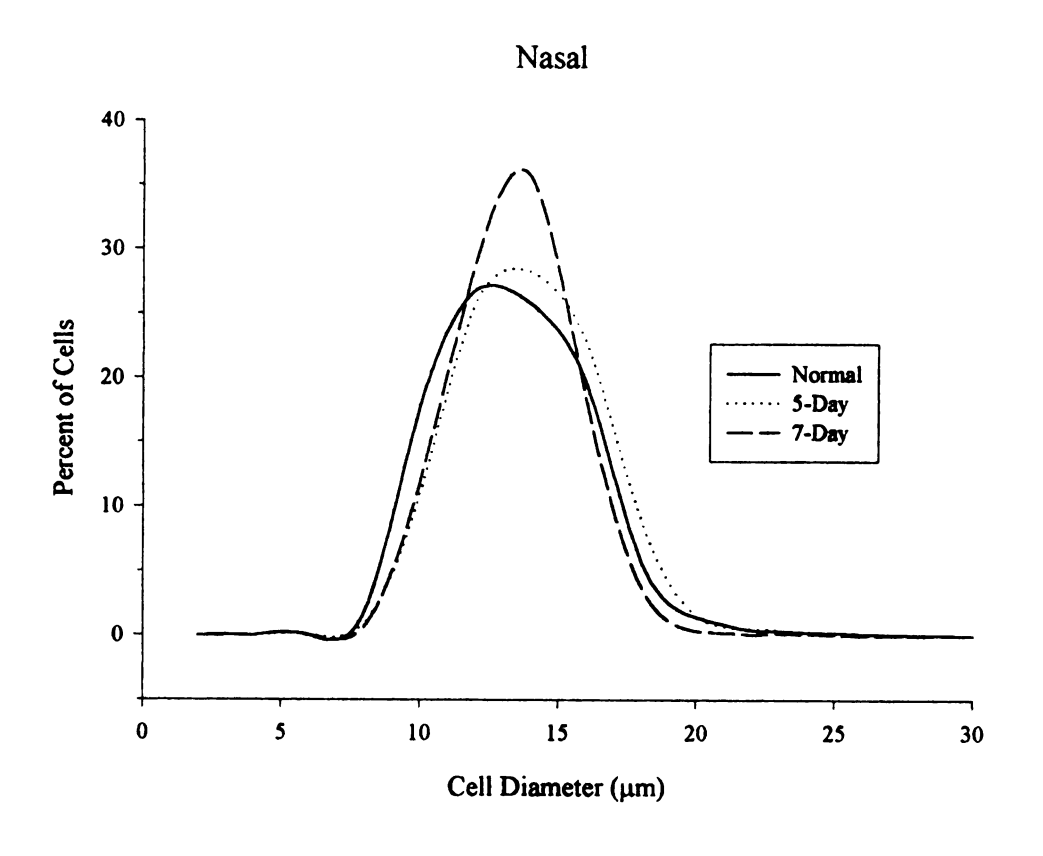


Figure 4. Histograms comparing the mean soma diameters of retinal ganglion cells in matched nasal and temporal regions of normal and TPP-treated ferrets 5 and 7 days after treatment. Mean soma size was similar for all groups (Kruskal-Wallis w/Mann Whitney).

Figure 5. Smoothed histograms showing the size distributions of retinal ganglion cells from matched nasal and temporal regions of the retinae in normal and TPP-treated ferrets 5 and 7 days after treatment. The cell size distributions were similar for all groups (Kolmogorov-Smirnov test).



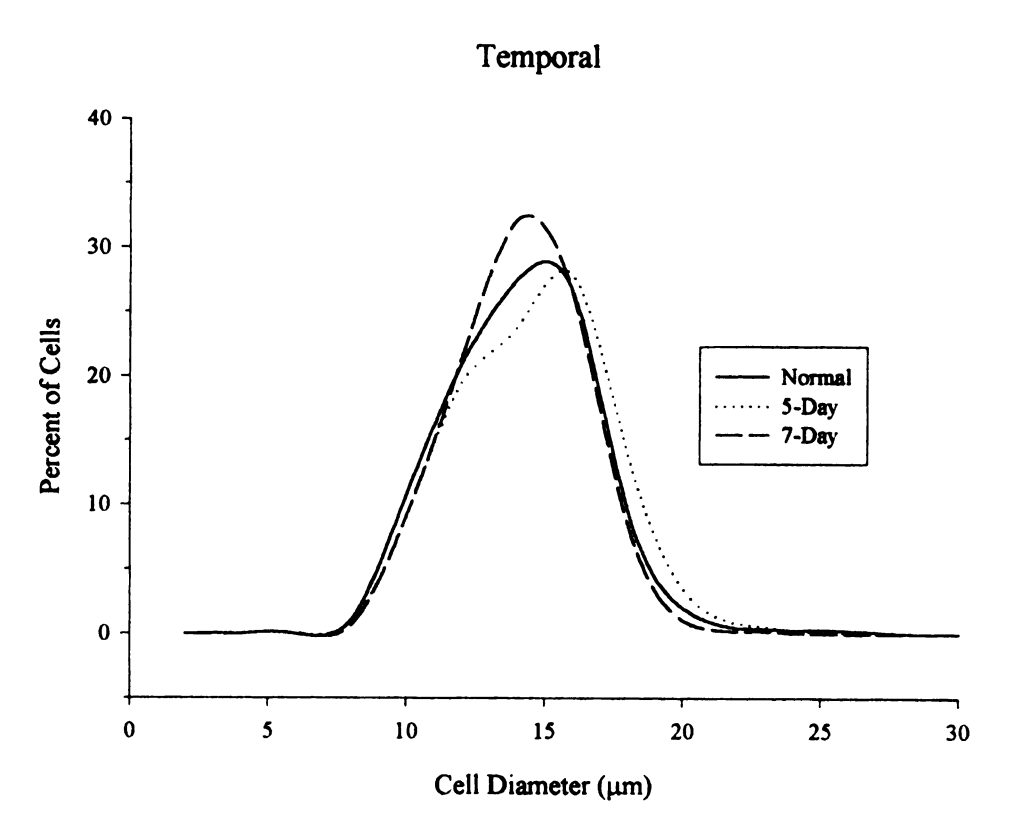
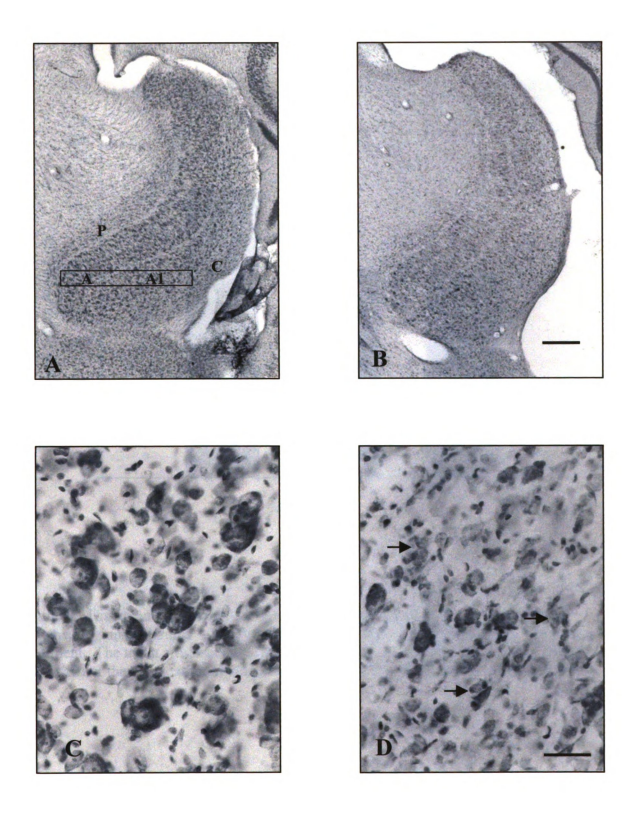


Figure 6. Photomicrographs of cresyl-violet stained parasagittal sections of the ferret LGN. (A) Low power (4x) view illustrating the laminar divisions C, A1, A, and the perigeniculate nucleus (P). (B) Low power view of a 5-day post-treatment LGN. Note the pale appearance of the TPP-treated LGN compared to normal. Scale bar = $50 \mu m$. (C) High power (40x) view of neurons in lamina A1 of a normal LGN. (D) High power view of neurons in lamina A1 of a 5-day post-treatment LGN. Note the irregular shaped, fragmented, pale staining, and pyknotic nuclei (arrows) in the TPP-treated in comparison to normal. Scale bar = $500 \mu m$.



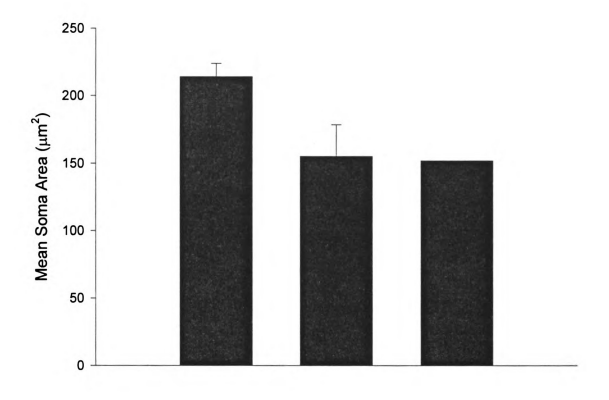


Figure 7. Histogram comparing the mean cross-sectional area in LGN neurons from matched regions in lamina A and A1 in normal and TPP-treated ferrets 5 and 7 days after treatment. The mean cross-sectional areas of LGN neurons in TPP-treated ferrets were 30% smaller than those of normal ferrets (* $\,$ p < 0.05 Kruskal-Wallis w/Mann Whitney).

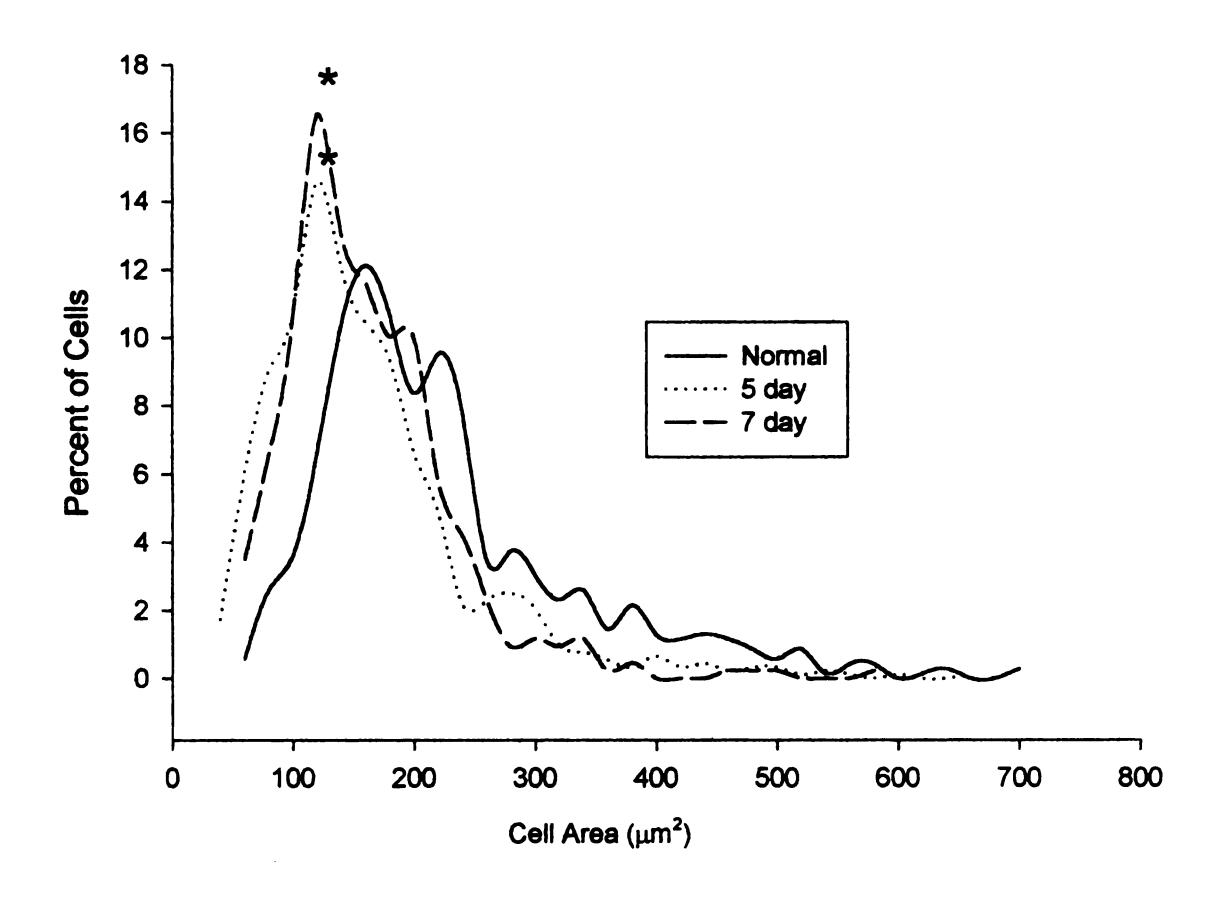
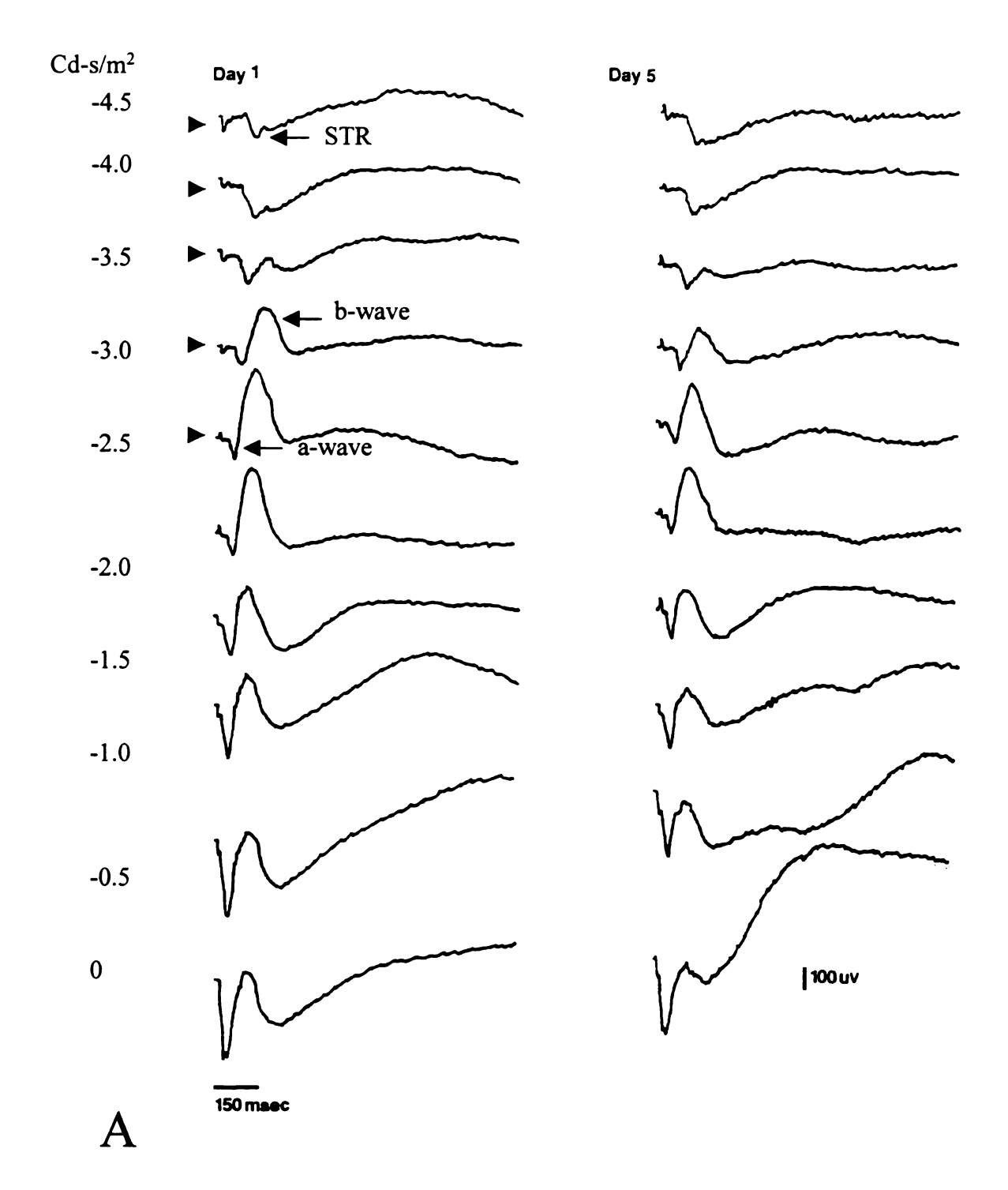
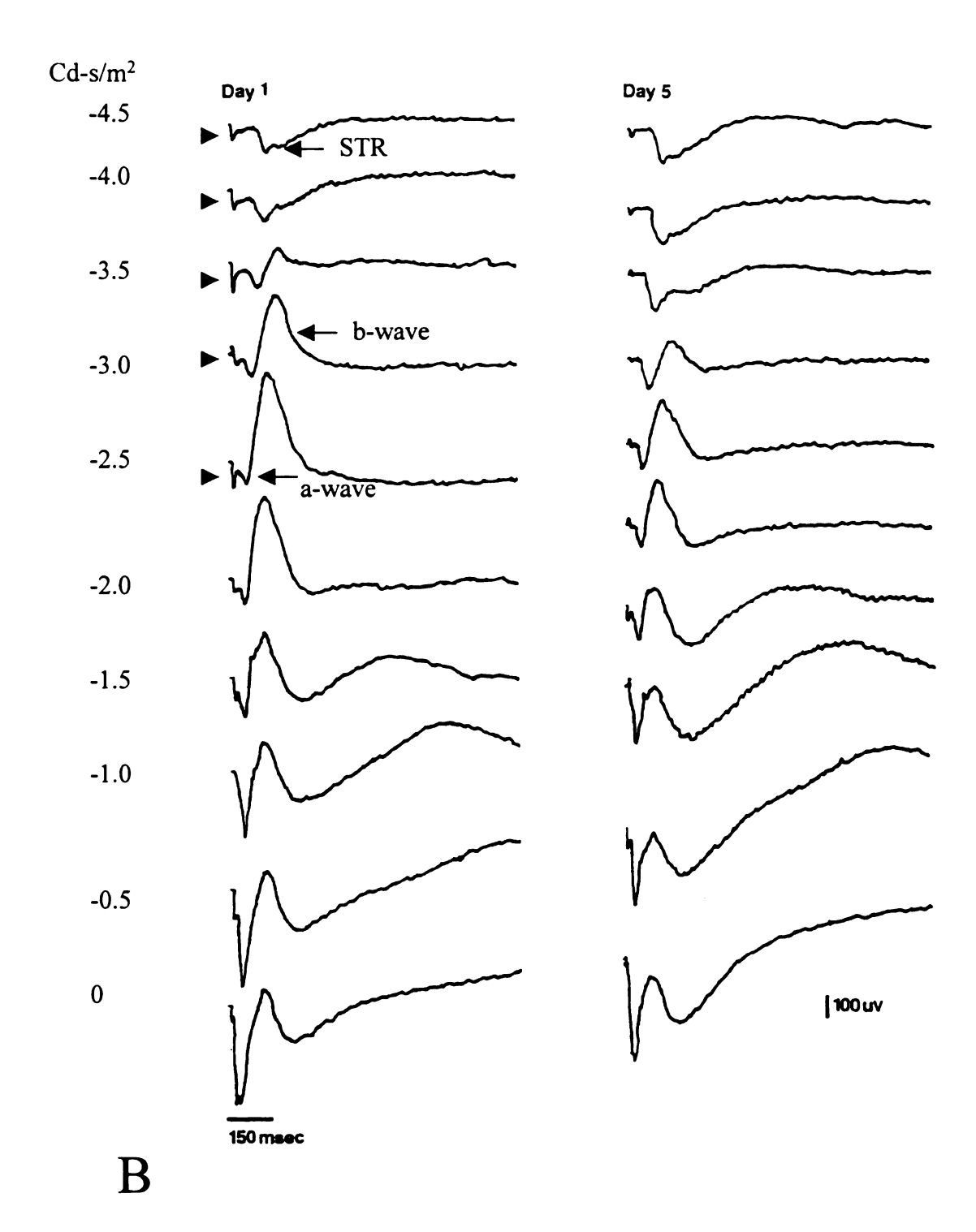


Figure 8. Smoothed histograms comparing the size distributions of neurons from matched regions in lamina A and A1 of the LGN in normal and TPP-treated ferrets 5 and 7 days after treatment. There was a significant shift toward smaller soma sizes in the TPP-treated ferrets compared to normal (* p < 0.05, Kolmogorov-Smirnov test).

Figure 9. Corneal ERG responses. (A) Responses from a normal ferret using a DTL fiber electrode at each stimulus intensity on day 1 and day 5. The STR, b-wave, and a-wave are labelled with arrows. The arrowheads point out the artifact. (B) Responses from a 5-day post-treatment ferret using a DTL fiber electrode at each stimulus intensity on day 1 before treatment and day 5 after treatment. The STR, b-wave, and a-wave are labelled with arrows. The arrowheads point out the artifact.





BIBLIOGRAPHY

BIBLIOGRAPHY

Abou-Donia MB. Organophorus ester-induced delayed neurotoxicity. *Annu Rev Pharmacol Toxicol* 1981;21:511-548.

Abou-Donia MB, Lapadula DM. Mechanisms of organophosphorus ester-induced delayed neurotoxicity: type I and type II. *Annu Rev Pharmacol Toxicol* 1990;30:405-440.

Abou-Donia MB. Triphenyl phosphite: A type II organophosphorous compound-induced delayed neurotoxic agent. In: J. E. Chambers and P. E. Levi, eds. *Organophophates: Chemistry, Fate and Effects.* San Diego: Academic Press, 1992;327-351.

Albensi BC. Apoptosis and biochemical cascades. Drug News Perspect 1999;12:1-5.

Baron RL. Delayed neurotoxicity and other consequences of organophosphorous esters. Annu Rev Entomol 1981;26:29-48.

Berends F. Mechanisms of ageing of organophosphate-inhibited esterases. In: F. De Matteis and E. A. Lock, eds. *Selectivity and Molecular Mechanisms of Toxicity*. New York: Macmillan Publishing Company, 1987;125-152.

Bien A, Seidenbecher CI, Bockers TM, Sabel BA, Kreutz MR. Apoptotic versus necrotic characteristics of retinal ganglion cell death after partial optic nerve injury. *J Neurotrauma* 1999;16:153-163.

Boyes WK, Tandon P, Barone JS, Padilla S. Effects of organophosphates on the visual system of rats. *J Appl Toxicol* 1994;14:135-143.

Brown KT, Wiesel TN. Localization of origins of electroretinogram components by intraretinal recording in the intact cat eye. *J Physiol* 1961;158:257-280.

Bush RA, Hawks KW, Sieving PA. Preservation of inner retinal responses in the aged royal college of surgeons rat. Evidence against glutamate excitotoxicity in photoreceptor degeneration. *Invest Ophthalmol Vis Sci* 1995;36:2054-2062.

Carroll EW, Wong-Riley MTT. Quantitative light and electron microscopic analysis of cytochrome oxidase-rich zones in the striate cortex of the squirrel monkey (Saimiri sciureus). *J Comp Neurol* 1984;222:1-17.

Cowan WM. Anterograde and retrograde transneuronal degeneration. In: W. J. H. Nauta and S. O. E. Ebbesson, eds. *Contemporary Research Methods in Neuroanatomy*. New York: Springer-Verlag, 1970;217-251.

Dowling JE, Ripps H. Adaptation in skate photoreceptors. *J Gen Physiol* 1972;60:698-719.

Dowling JE. The Retina: An Approachable Part of the Brain. Cambridge: Harvard University Press, 1987.

Ecobichon DJ. Organophosphorus ester insecticides In: D. J. Ecobichon and R. M. Joy, eds. *Pesticides and Neurological Diseases*. 2nd ed. Boston: CRC Press, 1994;171-249.

Ehrich M. Neurotoxic esterase inhibition: Predictor of potential for organophosphorus-induced delayed neuropathy. In: J. N. Blancato, R. N. Brown, C. C. Dary and M. A. Saleh, eds. *Biomarkers for Agrochemicals and Toxic Substances*. Washington, DC: American Chemical Society, 1996;79-93.

Fitzgibbon T, Wingate RJ, Thompson ID. Soma and axon diameter distributions and central projections of ferret retinal ganglion cells. *Vis Neurosci* 1996;13:773-786.

Frishman LJ, Shen FF, Du L, Robson JG, Harwerth RS, Smith EL, Carter-Dawson L, Crawford ML. The scotopic electroretinogram of macaque after retinal ganglion cell loss from experimental glaucoma. *Invest Ophthalmol Vis Sci* 1996;37:125-141.

Greiner JV, Weidman TA. Histogenesis of the ferret retina. Exp Eye Res 1981;33:315-332.

Hutchins JB, Casagrande VA. Development of the lateral geniculate nucleus: Interactions between retinal afferent, cytoarchitectonic, and glial process lamination in ferrets and tree shrews. *J Comp Neurol* 1990;298:113-128.

Imai H. Toxicity of organophosphorous pesticde (Fenthion) on the retina: Electroretinographic and biochemical study. *Acta Soc Ophthalmol Jpn* 1974;78:163-172.

Imai H, Miyata M, Uga S, Ishikawa S. Retinal degeneration in rats exposed to an organophosphate pesticide (Fenthion). *Environ Res* 1983;30:453-465.

Jackson CA, Peduzzi JD, Hickey TL. Visual cortex development in the ferret. I. Genesis and migration of visual cortical neurons. *J Neurosci* 1989;9:1242-1253.

Jamal GA. Neurological syndromes of organophosphorus compounds. Adverse Drug React Toxicol Rev 1997;16:133-170.

Johnson MK. Improved assay of neurotoxic esterase for screening organophosphates for delayed neurotoxic potential. *Arch Toxicol* 1977;37:113-115.

Johnson MK. The target for initiation of delayed neurotoxicity by organophosphorus esters: Biochemical studies and toxicological applications. In: E. Hodgson, J. R. Bend and R. M. Philpot, eds. *Reviews in Biochemical Toxicology*. New York: Elsevier, 1982;141-212.

Johnson MK. Organophosphates and delayed neuropathy- is NTE alive and well? *Toxicol Appl Pharmacol* 1990;102:385-399.

Joo CK, Choi JS, Ko HW, Park KY, Sohn S, Chun MTT, Oh YJ, Gwag BJ. Necrosis and apoptosis after retinal ischemia: Involvement of NMDA-mediated excitotoxicity and p53. *Invest Ophthalmol Vis Sci* 1999;40:713-720.

Kageyama GH, Wong-Riley MTT. Light and E.M. localization of cytochrome oxidase staining in the lateral geniculate nucleus. Soc Neurosci Abstr 1982;8:208.

Kageyama GH, Wong-Riley MTT. The histochemical localization of cytochrome oxidase in the retina and lateral geniculate nucleus of the ferret, cat, and monkey, with particular reference to retinal mosaics and ON/OFF-center visual channels. *J Neurosci* 1984;4:2445-2459.

Kamata R, Suzuki T, Saito S, Kofujita H, Ota M, Kobayashi H. Lack of correlation of organophosphorus-induced delayed neuropathy with neuropathy target esterase in hens and japanese quails. *J Health Sci* 1999;45:209-216.

Knoth-Anderson J, Abou-Donia MB. Differential effects of triphenyl phosphite and diisopropyl phosphorofluoridate on catecholamine secretion from bovine adrenomedullary chromaffin cells. *J Toxicol Environ Health* 1993;38:103-114.

Koelle GB. Pharmacology of organophosphates. J Appl Toxicol 1994;14:105-109.

Konno N, Katoh K, Yamauchi T, Fukushima M. Delayed neurotoxicity of triphenyl phosphite in hens: Pharmacokinetic and biochemical studies. *Toxicol Appl Pharm* 1989;100:440-450.

Kreft WD, Hoffert JR, Fromm PO. Action of organophosphates on the electroretinogram of rainbow trout. *Exp Biol* 1985;44:19-27.

Lehning EJ, Tanaka D, Jr., Bursian SJ. Triphenyl phosphite and diisopropyl phosphorofluoridate produce separate and distinct axonal degeneration patterns in the central nervous system of the rat. *Fundam Appl Toxicol* 1996;29:110-118.

Linden DC, Guillery RW, Cucchiaro J. The dorsal lateral geniculate nucleus of the normal ferret and its postnatal development. *J Comp Neurol* 1981;203:189-211.

Lotti M, Becker CE, Aminoff MJ. Organophosphate polyneuropathy: Pathogenesis and prevention. *Neurology* 1984;34:658-662.

Marrs TC. Organophosphate poisoning. Pharmac Ther 1993;58:51-66.

Peduzzi J. Relationship of geniculocortical afferents to developing neurons in the ferret visual cortex. Soc Neurosci Abstr 1988;14:743.

Richardson RJ. Assessment of the neurotoxic potential of chlorpyrifos relative to other organophosphorus compounds: A critical review of the literature. *J Toxicol Environ Health* 1995;44:135-165.

Sieving PA, Frishman LJ, Steinberg RH. Scotopic threshold response of proximal retina in cat. *J Neurophysiol* 1986;56:1049-1061.

Sieving PA, Wakabayashi K. Comparison of rod threshold ERG from monkey, cat and human. Clin Vis Sci 1991:6:171-179.

Stephans T. Organophosphate pesticides: Neurotoxins threaten farm workers. *The Journal of NIH Research* 1991;3:21-24.

Sultatos LG. Mammalian toxicology of organophosphorus pesticides. *J Toxicol Environ Health* 1994;43:271-289.

Tanaka D, Jr., Bursian SJ, Lehning EJ, Aulerich RJ. Exposure to triphenyl phosphite results in widespread degeneration in the mammalian central nervous system. *Brain Res* 1990;531:294-298.

Tanaka D, Jr., Bursian SJ, Aulerich RJ. Age-related effects of triphenyl phosphite-induced delayed neuropathy on central visual pathways in the European ferret (Mustela putorius furo). Fundam Appl Toxicol 1994;22:577-587.

Tanaka D, Jr., Lin M, Powell D, Morgan M, Lipsitz L, Aulerich RJ, Bursian SJ. Effects of dark-rearing on triphenyl phosphate-induced neuropathy in the visual system of the developing European ferret (Mustela putorius furo). *J Toxicol Environ Health* 1999;58:215-231.

Thompson EB. Special topic: Apoptosis. Annu Rev Physiol 1998;60:525-532.

Tian N, Slaughter MM. Correlation of dynamic responses in the ON bipolar neuron and the b-wave of the electroretinogram. *Vision Res* 1995;35:1359-1364.

U. S. EPA. Triphenyl Phosphite. CAS No. 101-02-0, Washington, D. C. 1985

Varghese RG, Bursian SJ, Tobias C, Tanaka D, Jr. Organophosphorus-induced delayed neurotoxicity: a comparative study of the effects of tri-ortho-tolyl phosphate and triphenyl phosphite on the central nervous system of the Japanese quail. *Neurotoxicology* 1995a;16:45-54.

Varghese RG, Bursian SJ, Tobias C, Tanaka D, Jr. Triphenyl phosphite-induced neuropathy in the avian forebrain: A silver impregnation study of the visual and auditory systems of the Japanese quail. *Neurotoxicology* 1995b;16:105-113.

Veronesi B, Dvergsten C. Triphenyl phosphite neuropathy differs from organophosphorus-induced delayed neuropathy in rats. *Neuropathol Appl Neurobiol* 1987;13:193-208.

Vitek DJ, Schall JD, Leventhal AG. Morphology, central projections, and dendritic field orientation of retinal ganglion cells in the ferret. *J Comp Neurol* 1985;241:1-11.

Voigt T, De Lima AD, Beckmann M. Synaptophysin immunocytochemistry reveals inside-out pattern of early synaptogenesis in ferret cerebral cortex. *J Comp Neurol* 1993;330:48-64.

Wakabayashi K, Gieser J, Sieving PA. Aspartate separation of the scotopic response (STR) from the photoreceptor a-wave of the cat and monkey ERG. *Invest Ophthalmol Vis Sci* 1988;29:1615-1622.

Wheater PR, Burkitt HG. Cell structure and function. Functional Histology. A Text and Colour Atlas. 2nd ed. New York: Churchill Livingstone, 1987;2-28.

Windebank AJ. Peripheral neuropathy due to chemical and industrial exposure. In: W. B. Matthews, ed. *Handbook of Clinical Neurology: Neuropathies*: Elsevier Science Publishers, 1987;263-292.

Wong ROL, Meister M, Shatz CJ. Transient period of correlated bursting activity during development of the mammalian retina. *Neuron* 1993;11:923-938.

Yoshikawa H, Yoshida M, Hara I. Electroretinographic changes induced by organophosphorous pesticdes in rats. *J Toxicol Sci* 1990;15:87-95.

Zahs KR, Stryker MP. The projection of the visual field onto the lateral geniculate nucleus of the ferret. *J Comp Neurol* 1985;241:210-224.

